Journal of Molecular Liquids 362 (2022) 119786

Contents lists available at ScienceDirect

Journal of Molecular Liquids

journal homepage: www.elsevier.com/locate/molliq

Kinetics and adsorption assessment of 1, 4-dioxane from aqueous solution by thiol and sulfonic acid functionalized titanosilicate

Mohammed Saeed Alamri [a], Hassan M.A. Hassan [a], Mosaed S. Alhumaimess [a], Abdullah M. Aldawsari [b], Ahmed A. Alshahrani [c], Thamer S. Alraddadi [d], Ibrahim Hotan Alsohaimi [a,*]

[a] Chemistry Department, College of Science, Jouf University, Sakaka 2014, Saudi Arabia
[b] Chemistry Department, College of Arts & Science, Wadi Al-dawaser, Prince Sattam Bin Abdulaziz University, Alkharj, Saudi Arabia
[c] National Centre for Technology Radiological Applications, King Abdul Aziz City for Science and Technology, Riyadh 11442, Saudi Arabia
[d] Department of Chemistry, College of Sciences and Arts-Alkamil, University of Jeddah, Jeddah 23218, Saudi Arabia

ARTICLE INFO

Article history:
Received 7 June 2022
Revised 30 June 2022
Accepted 3 July 2022
Available online 6 July 2022

Keywords:
1,4-dioxane
Water treatment
Adsorption
Sulfonic acid
Titanosilicate

ABSTRACT

In this work, thiol (-SH) and sulfonic acid (-SO_3H) groups post grafted on Titanosilicate (TS-SH, TS-SO_3H) was successfully prepared and efficiently used for the remediation of 1, 4 dioxane from aqueous medium employing batch experiments. The non-chemical interaction between the dioxane molecules and the titanosilicate surface plays a vital role in the remediation process, and the surface porosity can significantly boost the adsorption performance. The surface area of TS is 122 m^2/g and decreases to 110 and 95 m^2/g for TS-SH and TS-SO_3H, respectively, while the pore volume declines from 0.213 cm^3/g to 0.193 and 0.184 m^3/g for the same samples. The results revealed that TS-SH follows the Freundlich isotherm (R^2 = 0.9954), while TS-SO_3H follows the Langmuir isotherm (R^2 = 0.9963). The Langmuir removal capacity of TS-SO_3H for dioxane was found to be 164 mg/g. The adsorption kinetics for dioxane fits Pseudo second-order (PSO) and intraparticle diffusion (IPD). Such models suggest that particle diffusion and columbic interactions governed the adsorption characteristics. The desorption of dioxane using low concentration of HNO_3 resulted in a considerable regeneration performance. The adsorption of dioxane on TS-SH and TS-SO_3H was 98%, and 96%, respectively, reduced to 55%, and 75%, after four consecutive adsorption cycles.

1. Introduction

1,4-Dioxane is a new pollutant that is often employed as a stabilizer in the chlorinating solvent industries, notably in the production of tri-chloroethane. Although tri-chloroethane was forbidden in 1990 by Paris Agreement, 1,4-dioxane is a high-volume compound utilized in the manufacture of several everyday products, personal care, and pharmaceuticals as well as an inadvertent by-product of the production of plastic [1]. 1,4-Dioxane is a stubborn environmental pollutant that has been discovered in both surface and groundwater [2,3] with typical levels ranging from 10 – 1000 g/L, but as much as 100,000 g/L at some polluted groundwater locations [3]. Historically, this run ether was utilized as a solvent stabilizer for various chlorinated solvents [4]. Furthermore, 1,4-dioxane is a by-product of the manufacturing of polyester, plastics, and soap. Because 1,4-dioxane is extremely versatile and durable in the environment due to its chemical features, there is a considerable risk of human exposure [5], demanding effective separation of 1,4-dioxane from polluted locations to protect public health. To uptake 1, 4-dioxane from aquatic environment, numerous strategies such as biodegradation process, adsorption, and chemical oxidation were examined [6]. While chemical oxidation has indeed been extensively explored for the remediation of 1, 4-dioxane, it can yield hazardous transition products or necessitate huge amounts of chemicals and energy [7–9]. 1,4-dioxane biodegradation was also well investigated for bacterial pristine [10–13] and blend cultures [6,14], in the existence of co-pollutant containing chlorinated species [15,16].

Adsorption is the most appropriate approach for organic contaminants removal due to its low-cost, high performance, simplicity, and lack of secondary contamination. Numerous adsorbents comprising activated carbon and [17] the polymeric materials [18,19] were examine to uptake 1,4-dioxane from aquatic environment, but few were noted to offer sufficient amount for economically-viable site cleanup implementation. However, these adsorbents exhibit several limitations, such as pore size distribution and nonspecifically of adsorbents.

* Corresponding author.
E-mail address: ehalshaimi@ju.edu.sa (I. Hotan Alsohaimi).

https://doi.org/10.1016/j.molliq.2022.119786
0167-7322/

Titanosilicate (TS) was synthesized as a novel type of zeolite with unique features such as strong hydrophobic nature and selectivity [20], indicating its promise for chemical separation implementations. Chen and coworkers fabricated a membrane of TS and examined its separation performance for mixtures of ethanol/water [21], and the findings revealed good selectivity for ethanol in the mixture. Temperature programmed desorption methods were utilized by Serrano et al., to establish preferential adsorptions of organic compounds in water-comprising flows on titanium centers with great hydrophobic indices [22]. The processes of adsorption of common hydrocarbon on diverse kinds of zeolites were thoroughly studied. Mellot demonstrated the textural and energies of hydrocarbon adsorption centers in zeolite, leading to the conclusion that typical hydrocarbon uptake in zeolites comprises H-bonding with the framework oxygens [23]. To date, the uptake of 1,4-dioxane on conventional adsorbents, like pure and modified titanosilicate is not yet well investigated, and the various parameter regulating the performance removal of 1,4-dioxane are not completely known. The tailoring of thiol and sulfonic acid groups on titanosilicate (TS) can enhance the removal performance of dioxane from aqueous environment.

According to the literature citation, there is no explication for dioxane adsorption on modified titanosilicate (TS) adsorbent with thiol (-SH) and sulfonic acid (-SO_3H), and there is no data on modified TS for dioxane adsorption. This is the first time an adsorption process has been investigated employing a TS adsorbent modified with thiol (-SH) and sulfonic acid (-SO_3H) moieties. Therefore, the purpose of this work is to look into the fundamental adsorption process of pure TS, TS-SH (thiol functionalized TS), and TS-SO_3H (sulfonic acid functionalized TS) for the adsorption of 1,4-dioxan from aqueous medium. A set of adsorption tests were conducted to investigate the adsorption behavior and the effects of various parameters (pH, contact time, dose, and concentration).

2. Experimental

2.1. Materials

NaOH (≥98%), 1,4-dioxane (99.8%), (3-Mercaptopropyl) trimethoxysilane (MPTEOS, 95%), tetrabutyl titanate (TBOT, 97%), tetrapropylammonium hydroxide (TPAOH, 1.0 M in H_2O), tetraethyl orthosilicate (TEOS, 98%), hydrogen peroxide (H_2O_2, 35%), HCl (37%), Sodium Sulphite (≥98%), and ethanol (95%) were procured from Sigma-Aldrich Co., USA. Toluene (99.9%) was provided from Scharlau, Spain. Sodium disulfite were obtained from BDH Chemicals Ltd. Poole, England. 1-Amino-2-naphthol-4-sulphonic acid (95%) was supplied by Acros organics (Belgium). All materials were used in their natural state, with no further processing. The Milli-Q direct 8 purification system was employed to get the deionized water (DI) used in all of the tests (Millipore, France).

2.2. Materials synthesis

2.2.1. Hydrothermal preparation of titanium silicate composite (TS)

The hydrothermal synthesis approach was utilized to develop TS, as described in previous study [24]. The materials ratio was TEOS: TBOT: TPAOH: H_2O = 15: 0.23: 7.35: 17.5, and the blend was agitated at 50 °C until a homogenous solution is obtained. The solution was then heated at 80 °C to eliminate alcohol before being transferred into Teflon autoclave followed by heating for 24 h at 170 °C. The obtained product was centrifuged, rinse with distilled water and vacuum dried overnight. To eliminate the organic framework, the white powder was calcined at 550 °C for 10 h.

2.2.2. Preparation of thiol and sulfonic acid modified TS

TS-SO_3H were fabricated through a combination between hydroxyl moieties present on TS and MPTEOS followed by in situ oxidation utilizing a solution of H_2O_2 (30 wt%) (Scheme 1) [25]. TS (1 g) were typically was suspended utilizing a sonicator in toluene (50 ml) for 2 h. The TS dispersion was transferred into a round-bottom flask, followed by the gentle addition of MPTEOS (1.5 ml). The obtained suspension was then refluxed at for 24 h 105 °C. TS-SH were developed, and then separated and thoroughly washed with toluene, ethanol and water–ethanol mixture followed by vacuum dried at 100 °C. TS thiol (–SH) moieties were changed to sulfonic acid (–SO_3H) by a moderate oxidation process utilizing H_2O_2 (40 ml, 35%) for 24 h at ambient temperature. The sulfonic acid-functionalized TS-SO_3H was separated and rinsed several times with ethanol and DI water before drying in an 80 °C vacuum oven.

2.3. Physicochemical characterization

Fourier transform infrared (FTIR) spectra were recorded using Shimadzu IR Tracer-100 (Shimadzu, 1 Nishinokyo Kuwabara-cho, Nakagyo-ku, Kyoto 604–8511, Japan) in the range of 4000–400 cm^{-1} to validate the modification of TS. Using Shimadzu diffractometer (XRD7000), X-ray diffraction (XRD) were carried out using Cu-Kα radiation (1.54056 Å) at 40 kV and 40 mA. Thermogravimetric analysis (TGA) profiles (25–600 °C, 10 °C min^{-1}, under flowing air gas) were done on a Shimadzu TGA-51. A NOVA-4200e (Quantachrome Instruments, Quantachrome GmbH & Co. KG, Boynton Beach, USA) was utilized to acquire the N_2 isotherms and surface properties at −196 °C. The pore size distributions were determined using the Barrett–Joyner–Halenda (BJH) technique using the adsorption branch of the nitrogen isotherms. The morphology was evaluated utilizing the field emission scanning electron microscope (FESEM, thermo Scientific Quattro ESEM, Thermo Fisher, Waltham, MA, USA). The UV–vis spectra were obtained on a UV Visible spectrophotometer Agilent Cary 60 Spectrophotometer (Agilent Technologies, USA).

2.4. Batch experiment

To best explain the adsorption behavior of TS, TS-SH, and TS-SO_3H for 1,4-dioxane, varying factors such as pH (2.5–9.4), initial concentration of dioxane (25–300 ppm), contact time (1–420 min), and adsorbent dose (0.01–0.05 g), adsorption/desorption experiments were investigated. Following the analysis of these variables, the concentration of the residual dioxane was assessed utilizing UV–Visible spectrophotometer Agilent Cary 60 Spectrophotometer (Agilent Technologies, USA) [26], and the adsorption (%) and uptake capacity are estimated utilizing the following Equations (1)–(3)

$$\text{Removal}\,(\%) = \frac{(C_i - C_e)}{C_i} \times 100 \quad (1)$$

$$\text{Adsorption Capacity}\,(q_e) = \frac{V(C_i - C_e)}{m} \quad (2)$$

$$q_t = \frac{V(C_i - C_t)}{m} \quad (3)$$

where m, v, C_i, C_t, C_e, q_t, and q_e are the dose of adsorbent (g), dioxane volume (L), initial dioxane concentration at certain time, equilibrium concentration, adsorption capacity at C_t and adsorption capacity at C_e, respectively.

Kinetic models explain the adsorption mechanism as well as the reaction order. The dioxane removal process is considerably time-dependent and influenced by the physicochemical characteristics

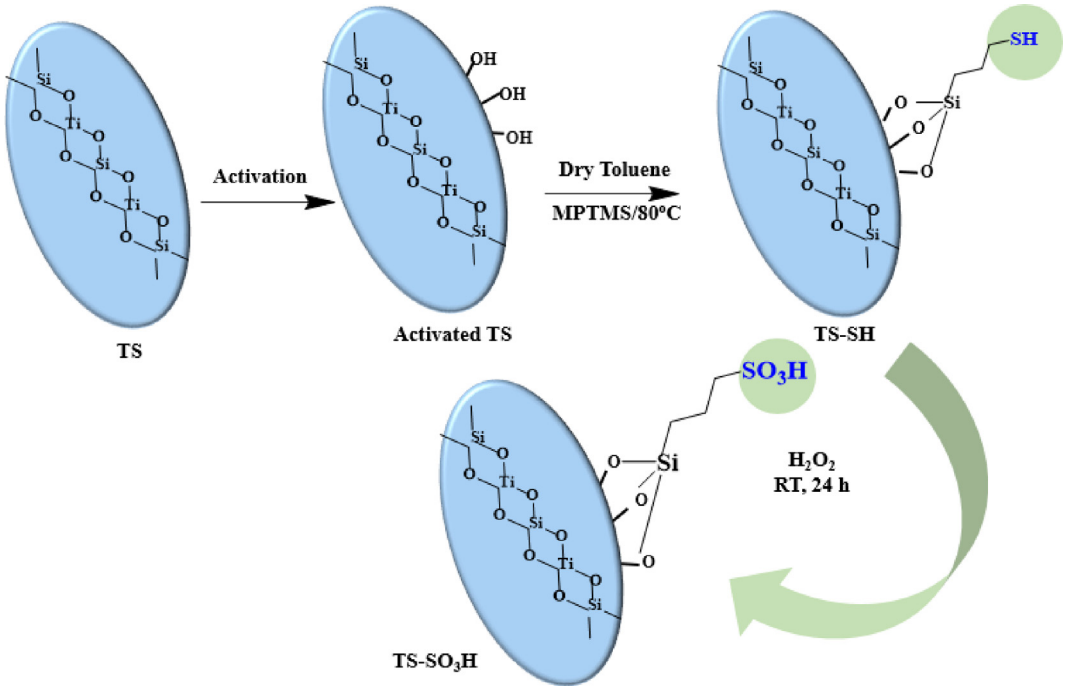

Scheme 1. . Schematic representation displaying the synthesis of TS-SO_3H.

of pure TS and modified TS. Four distinct kinetic models such as Elovich, intraparticle diffusion (IPD), pseudo second-order (PSO), and pseudo first-order (PFO) were utilized to evaluate the various kinetic variables to investigate the removal mechanism. The four kinetic models were provided using the following Eqs. (4)–(7):

$$\text{Elovich } q_t = \left(\frac{1}{\beta}\right)\ln(\alpha x \beta x t) + \left(\frac{1}{\beta}\right)\text{Ln } t \quad (4)$$

$$\text{IPD } \quad q_t = k_i \, x \sqrt{t} \, x \, X_i \quad (5)$$

$$\text{PSO } \quad \frac{t}{q_t} = \frac{1}{(k^2 \, x \, q_e^2)} + \frac{t}{q_t} \quad (6)$$

$$\text{PFO } \ln(q_e - q_t) = \ln q_e - k_1 t \quad (7)$$

Adsorption models describe the adsorption mechanism, adsorbate interaction mode with adsorbent, and adsorption capacity. The most generally used models were utilized to analyze the removal process, as presented in Eqs. (8)–(10):

$$\text{Langmuir } \frac{1}{q_e} = \frac{1}{(q_m \, x k_L \, x C_e)} + \frac{1}{q_m} \quad (8)$$

$$\text{Freundlich } \quad \ln q_e = \ln K_f + \frac{1}{n}\ln c_e \quad (9)$$

$$\text{Temkin } q_{e=} \, BT \, x \ln(ATx C_e) \quad (10)$$

2.5. Desorption studies

For the desorption measurements, 20 mg of the TS-SO_3H was introduced to 50 ml of dioxane solution and the dispersion was then agitated for 2 h at 200 rpm. After that, the dioxane saturated TS-SO_3H was separated. Then, the adsorbent was introduced into 25 ml of 1 M HCl, 1 M NaOH, 1 M HNO_3, with continuous stirring for 120 min. The TS-SO_3H was separated from the solution and recycled for adsorption again. The solution was determined by UV visible to determine the concentration of the eluted dioxane. The % desorption of the dioxane was determined as:

$$\%\textbf{Desorption} = \frac{\text{concentration of dioxane eluted by 1M HCl}}{\text{Initial concentration of dioxane captured on TS} - \text{SO3H}} \text{ x } 100 \quad (11)$$

3. Results and discussion

3.1. Characterization of the fabricated materials

3.1.1. Spectroscopic characterization

FTIR spectra of TS, TS-SH, and TS-SO_3H are illustrated in Fig. 1. The wide characteristic band in the range from 3100 to

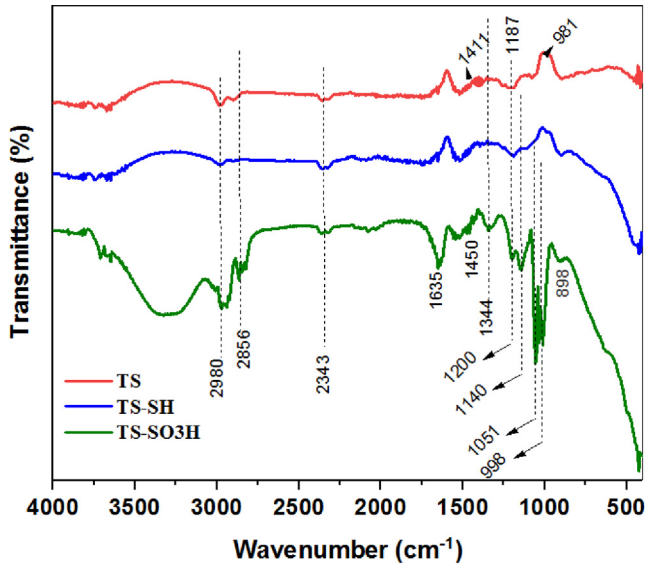

Fig. 1. FTIR spectra of TS, TS-SH, and TS-SO_3H materials.

3435 cm^{-1} are ascribed to the stretching mode of O–H moieties on TS, TS-SH, and TS-SO_3H. The peaks at 1635 cm^{-1} are ascribed to Ti-O-Ti stretching present in all fabricated samples [27]. In the FTIR spectrum, the peaks at 1344 and 1140 cm^{-1} are attributed to S = O and the band at 1051 cm^{-1} is ascribed to O = S = O stretching vibration. The characteristic bands of TS matrix at 981, 1187 and 1411 cm^{-1} which are related to the common Si-O-Ti, asymmetric stretching of Si-O-Si, and δ (zeolite) which were shifted to 998, 1200 and 1450 cm^{-1}, respectively [28–30]. The remarkable band shifts to greater wavenumbers for the TS-SO_3H, sulfonic acid modified TS confirmed the grafting of sulfonic acid moieties on TS through coupling and in situ oxidation process (Scheme 1).

XRD was used to characterize the crystallinity of the fabricated materials. The XRD patterns of TS, and TS-SO_3H in the 5 to 50° range are displayed in Fig. 2. Both developed materials had a characteristic MFI structure. Substantial peaks were shown at 2θ = 7.6°, 8.7°, 22.8°, 23.7° and 24.3°, which assigned to the five typical peaks of MFI structure [31]. Furthermore, the sole diffraction peak at 2θ = 29.5° were attributed to the Ti-atom that was integrated into the zeolite matrix [32]. Thus, the XRD results thus indicated a successful fabrication of TS, and the fabricated TS showed no noticeable changes in the crystal structure following modification with a sulfonic acid group. Meanwhile, the diffraction peaks of TS-SO_3H were more intense than those of TS, presumably indicating that TS-SO_3H has a larger crystal size.

3.1.2. Thermal stability

Thermogravimetric assessment (TGA) of TS, TS-SH, and TS-SO_3H was done using thermogravimetric analyzer in the temperature range of 50–600 °C at heating rate of 10 °C min^{-1} under N_2 atmosphere to determine the quantity of thiol (-SH) and sulfonic acid (-SO_3H) groups grafting in titanosilicate (TS). The obtained results is depicted in Fig. 3. The inclusion quantity of thiol/-SH and sulfonic acid/-SO_3H moieties in TS was calculated from the weight remain for TS, TS-SH, and TS-SO_3H at 600 °C applying the following equation.

$$The grafting amount of SH or SO3H(\%) = \frac{W_{TS} - W_{TS-SH or TS-So3H}}{W_{TS}} \times 100 \quad (12)$$

where W_{TS} is the weight of TS remaining (%) and $W_{TS\text{-}SH\ or\ TS\text{-}SO3H}$ is the weight of thiol/-SH and sulfonic acid/-SO_3H moities residue remain (%) at 600 °C. The grafting quantity of thiol (-SH) and sulfonic acid (-SO_3H) groups in TS was found to be 3.98% and 6.64%, respectively.

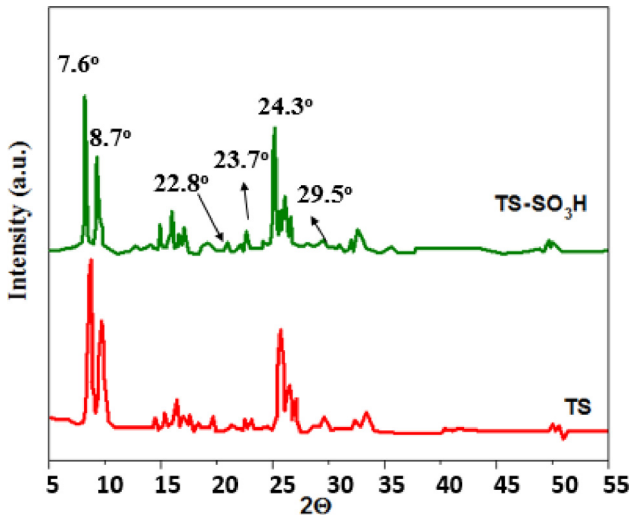

Fig. 2. XRD patterns of TS, and TS-SO_3H materials.

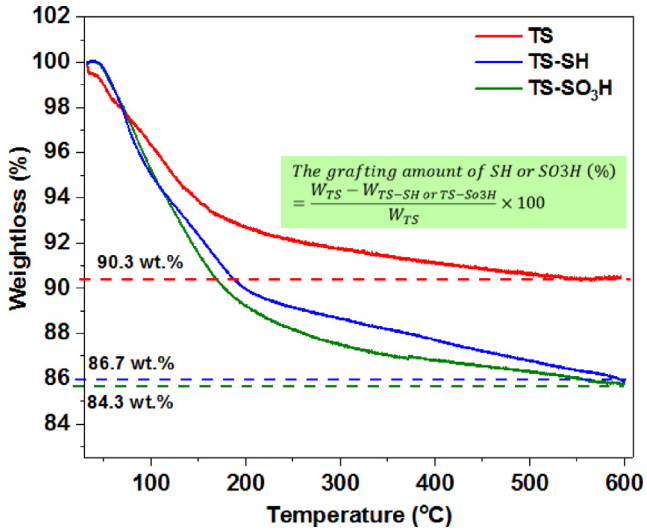

Fig. 3. TGA profiles of TS, TS-SH, and TS-SO_3H materials.

3.1.3. Surface and textural features

N_2 adsorption isotherms at (77 K) provided insights on the porosity and the textural properties of the prepared materials, allowing the determination of surface area, and pore volume. Fig. 4 depicts the N_2 isotherms and pore size distribution of TS, TS-SH, and TS-SO_3H. According to the International Union of Pure and Applied Chemistry (IUPAC) classification, all materials' isotherms were type IV with an H1 hysteresis loop, suggesting that all materials have well-defined mesoporous materials. Furthermore, all materials had a comparable isotherm shape, indicating that the initial pore structure of TS remained mostly constant following alteration with thiol (-SH) and sulfonic acid group (-SO_3H). The N_2 adsorption – desorption of the TS-SH and TS-SO_3H in comparison with that of pure TS indicated a considerable reduction in the N_2 adsorption; nevertheless, much greater N_2 uptake at the relative pressure of P/Po less than 0.02 is a characteristic of porous zeolites. The larger hysteresis loop with completion at the smaller P/Po of TS revealed more *meso*-porosity than that of TS-SH and TS-SO_3H. The surface area of pristine TS is 122 m^2/g and drops to 110 and 95 m^2/g for TS-SH and TS-SO_3H, respectively, while the pore volume drops from 0.213 cm^3/g to 0.193 and 0.184 m^3/g for the same samples. The significant reduction in surface area and pore volume might be attributed to the post grafting of the functional moieties as thiol or sulfonic acid moiety, which cause some pores to become partly occluded and inaccessible to nitrogen molecules. Moreover, The Pore size distribution of TS showed similar behavior to that of TS-SH and TS-SO_3H materials, with a distinct pore centered at 2.5 nm for all developed materials.

The morphology of the materials was inspected using FESEM on the developed materials, as seen in Fig. 5. The FESEM image of pristine TS revealed a narrow range of particle sizes as well as uneven morphology with rounded rectangular shapes. TS-SH and TS-SO_3H, on the other hand, had more homogeneous particle sizes and a more regular merged spherical and oval-like shape.

3.2. Batch adsorption investigations

3.2.1. Influence of pH

The solution's pH has a crucial influence on the uptake tendency of the fabricated adsorbents, which is dependent on the type of adsorbent in relation to the columbic interaction on

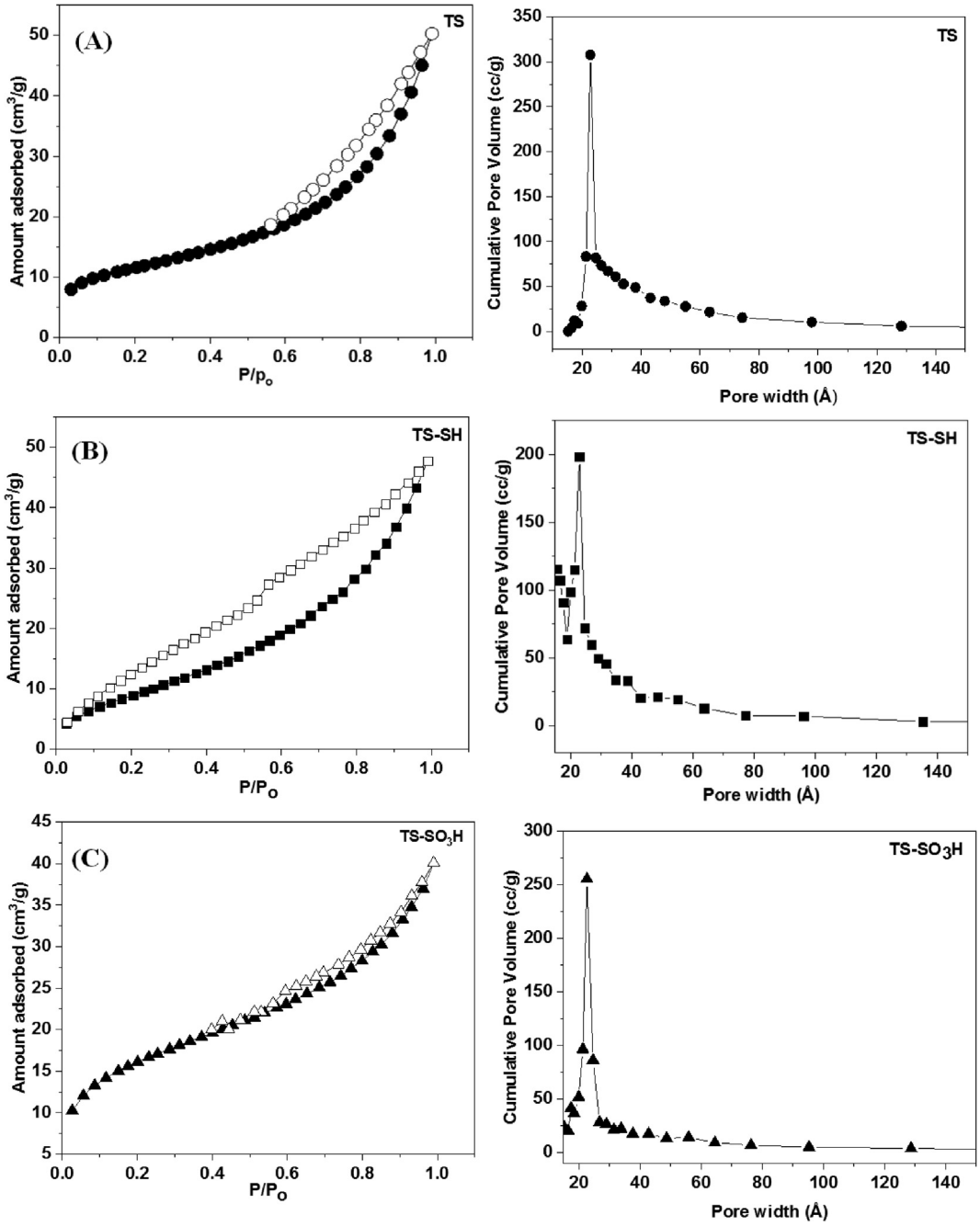

Fig. 4. N_2 adsorption–desorption isotherm at 77 K and pore size distribution of (A) TS, (B) TS-SH, and (C) TS-SO_3H materials.

the employed dioxane molecules. The influence of the dioxane solution's pH on the uptake process was assessed at pH level (2–10). The influence of the pH on the removal of 1,4 dioxane on TS-SH and TS-SO_3H adsorbents were tested while the other variables were constant (25 °C, 300 min, 5 mg), as presented in Fig. 6**a** and Fig. 7**a**, respectively. The results revealed that the removal capacity rises with increasing pH, reaches the highest at slightly basic pH for TS-SH sample (Fig. 6**a**) and neutral pH for TS-SO_3H (Fig. 7**a**), and then declines. The smaller removal capacity of both adsorbents was shown at small pH (2–5). An appropriate reason for minimal removal at small pH is the existence of greater quantities and high movement of H^+ ions that combine to water molecules to produce H_3O^+ (hydronium ions), so that the adsorption centers on the adsorbent's surface are covered by H_3O^+, restricting dioxane from attaining the adsorbent's binding centers [33]. A significant reduction in the dioxane adsorption performance was seen in high pH (greater than 9). This could be attributed to the development of OH^-(hydroxyl ions), which then compete with the dioxane molecules for removal centers, resulting in to a reduction in dioxane's removal performance [34]. Furthermore, the significant decrease in the uptake could be attributed to the generation of a negative charge on both adsorbents which may result in a repulsion effect with dioxane. Therefore, the optimum pH chosen for this work was 8.6 and 7.1 for TS-SH and TS-SO_3H, respectively.

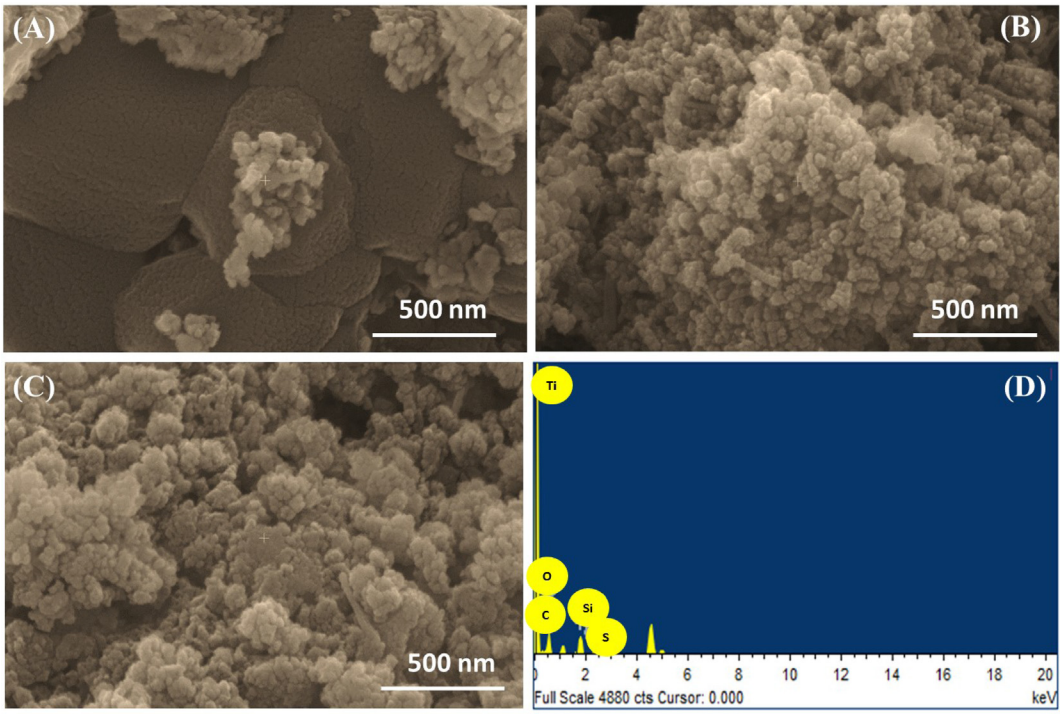

Fig. 5. FESEM of (A) TS, (B) TS-SH, (C) TS-SO_3H, and (D) EDX of TS-SO_3H.

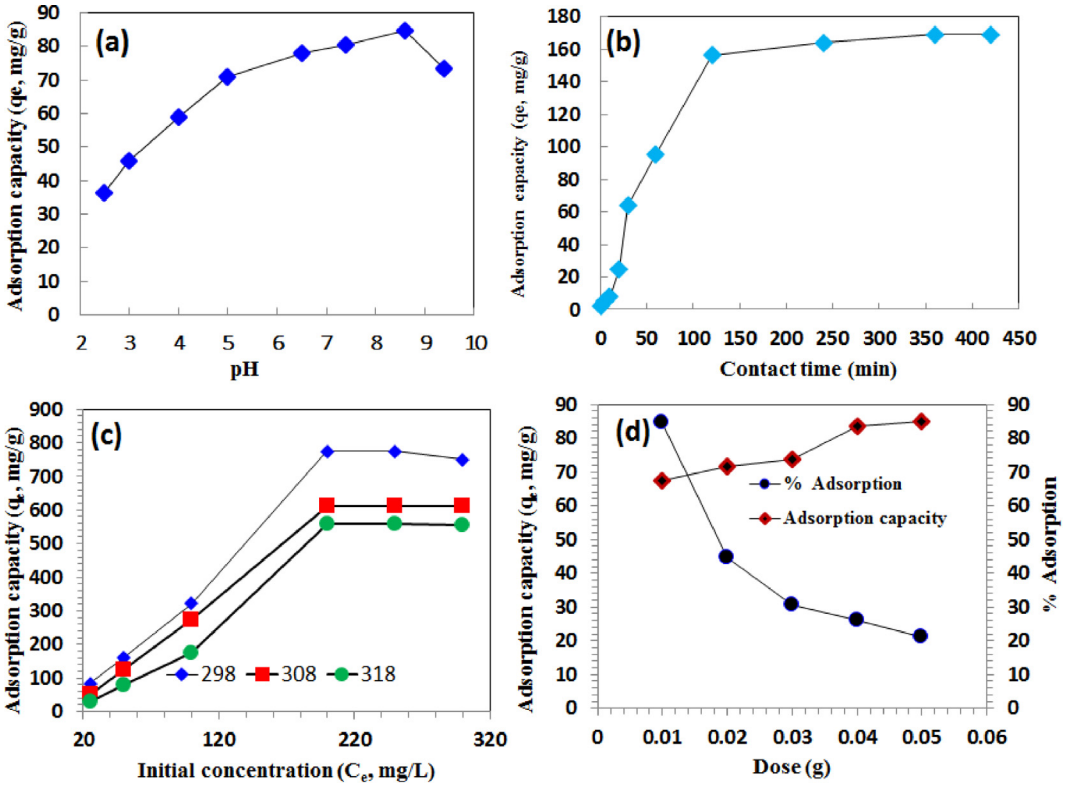

Fig. 6. (a) Effects of pH (25 ppm, 25 °C, 300 min, 5 mg); (b) effect of contact time (25 ppm, 25 °C, PH 8.6, 5 mg) (c) effect of initial concentration of dioxane (25 °C, 35 °C, and 45 °C, 5 mg, pH 8.6), (d) Effect of dose (25 °C, 300 min, 5 mg) on the removal capacities of dioxane over TS-SH material.

3.2.2. Influence of contact time

The impact of contact time is a critical component in determining the adsorbents' remediation performance. The effect of adsorbate/adsorbent contact time on the dioxane uptake properties of the utilized adsorbents (TS-SH and TS-SO_3H) was investigated throughout a range time interval (1–420 min), as depicted in Fig. 6**b** and Fig. 7**b**. The dioxane removal was seen immediately after the introducing of adsorbents, showing a rapid accessibility

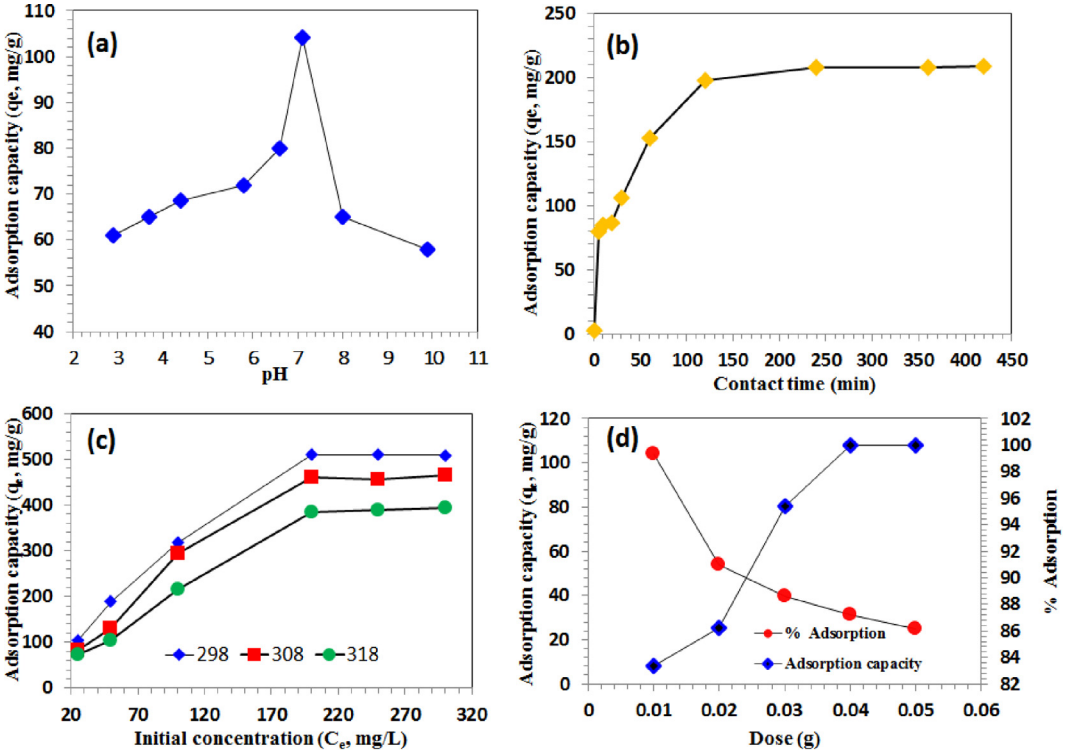

Fig. 7. (a) Effects of pH (25 ppm, 25 °C, 300 min, 5 mg); (b) effect of contact time (25 ppm, 25 °C, PH 8.6, 5 mg) (c) effect of initial concentration of dioxane (25 °C, 35 °C, and 45 °C, 5 mg, pH 8.6), (d) Effect of dose (25 °C, 300 min, 5 mg) on the removal capacities of dioxane over TS-SO_3H material.

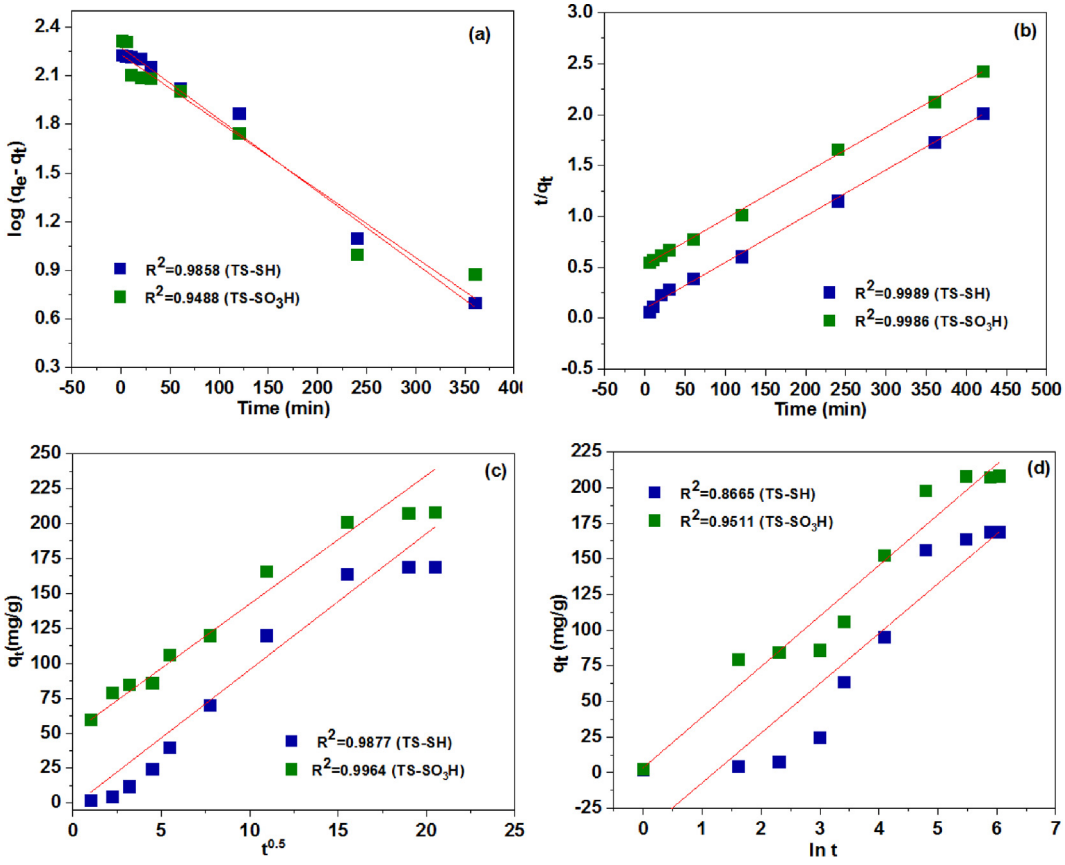

Fig.8. Kinetic model for adsorption of 1, 4 dioxane on TS-SH and TS-SO_3H (a) PFO, (b)PSO, (c)IPD, and (d)Elovich.

Table 1
Kinetics variables applying pseudo-first-order (PFO), pseudo-second-order (PSO), intraparticle diffusion (IPD), and Elovich of 1, 4 dioxane adsorption on TS-SH and TS-SO_3H.

PFO	TS-SH	TS-SO_3H	PSO	TS-SH	TS-SO_3H
k_1 (min^{-1})	0.005	0.004	k_2 (g mg^{-1} min^{-1})	0.006	0.009
q_e (mg/g)	156	188	q_e (mg/g)	173	221
R^2	0.9858	0.9488	R^2	0.9989	0.9989
IPD	TS-SH	TS-SO_3H	Elovich	TS-SH	TS-SO_3H
k_i(g mg^{-1} $min^{-0.5}$)	9.021	9.70	α	12.30	15.50
C_i (ppm)	2.065	50.5	β	0.029	0.028
R^2	0.9877	0.9964	R^2	0.8670	0.9511

of active centers for the dioxane remediation. An improve in the uptake of the dioxane was achieved as the contact time was prolonged and up to 70 % and 83.4% dioxane remediation was achieved with both TS-SH and TS-SO_3H within 360 and 240 min, respectively. The optimal contact time for dioxane and TS-SH was 360 min and 240 min for TS-SO_3H based on the maximal removal capabilities. These adjusted contact periods were then employed for the remainder of the remediation tests.

3.2.3. Influence of initial concentration of dioxane

The performance of dioxane remediation on TS-SH and TS-SO_3H adsorbents was tested in relation to the initial concentration of dioxane (25–300 mg/L) at pH 8.6 and 7.1 for both TS-SH and TS-SO_3H, respectively, (Fig. 6**c** and Fig. 7**c**). The remediation capability of dioxane was boosted from 84 to 750 $mg.g^{-1}$ and from 104 to 509 $mg.g^{-1}$ as the dioxane concentration raised from (25–300 mg/L) using TS-SH and TS-SO_3H, respectively. This might be connected to the fact that when the dioxane initial concentration was increased, a significant adsorption capacity was attained owing to the accessibility of empty adsorbed centers. Furthermore, the removal capability of both adsorbents diminishes as the temperature rises from 25 to 45 °C, indicating that the removal process is exothermic.

3.2.4. Influence of dose

The impact of the TS-SH and TS-SO_3H on the remediation of dioxane at ambient temperature with an initial dioxane concentration of 25 mg L^{-1} was examined as depicted in Fig. 6**d** and Fig. 7**d**. As the TS-SH and TS-SO_3H doses rose from 0.01 to 0.05 g, the capacity of remediation decreased while the performance of the uptake improved.

3.2.5. Kinetic studies

To fully grasp the kinetics of the remediation process, four distinct kinetic models were applied: pseudo-first-order (PFO) (Fig. 8**a**), pseudo-second order (PSO) (Fig. 8**b**), intraparticle diffusion (IPD) (Fig. 8**c**), and Elovich (Fig. 8**d**). The regression coefficient, R^2, reflected the agreement between experimental results and model predictions. A large R^2 value suggests that the kinetic model was well matched. The adsorption kinetics for dioxane remediation using both TS-SH and TS-SO_3H adsorbents based on the regression factor (R^2) fits Pseudo second-order (PSO) and intraparticle diffusion (IPD). Such models suggest that particle diffusion and columbic interactions governed the adsorption mechanism. The additional kinetic variables of various models are presented in Table 1.

3.2.6. Adsorption isotherms

To investigate the essential adsorption features of removal capacity and interaction, three adsorption isotherms: Freundlich (Fig. 9**a**), Langmuir (Fig. 9**b**), and Temkin (Fig. 9**c**) was applied. The arguments behind these isotherms were summarized in Table 2. The results revealed that TS-SH follows the Freundlich isotherm (R^2 = 0.9954), while TS-SO_3H follows the Langmuir isotherm

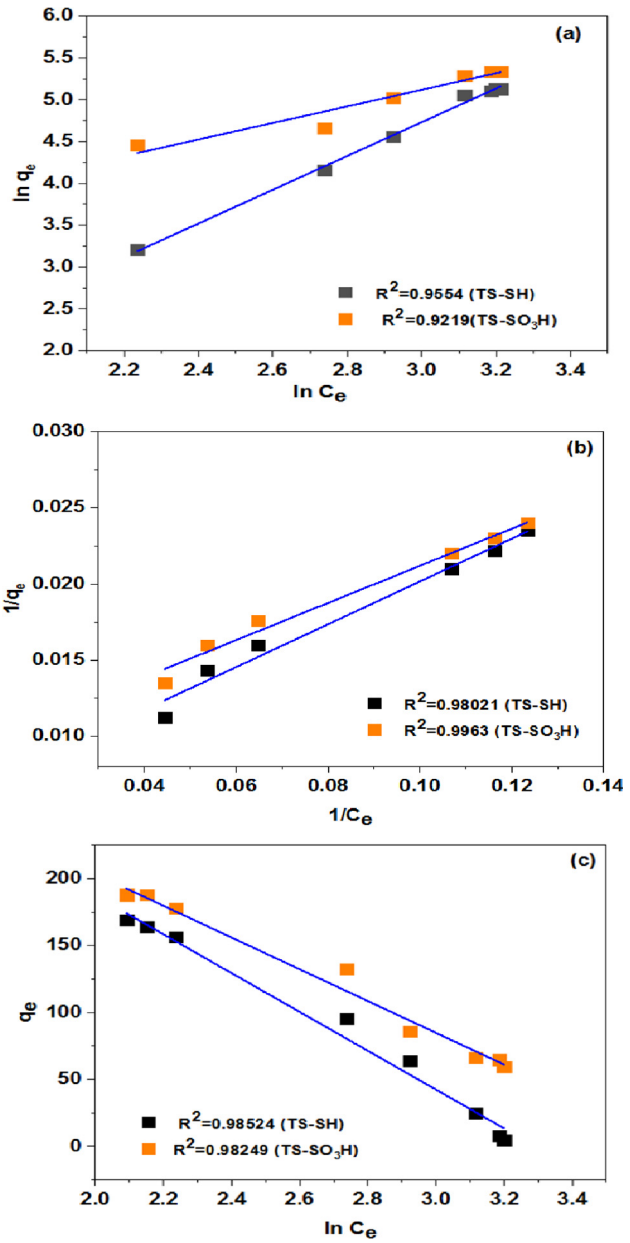

Fig.9. Adsorption isotherm model for adsorption of 1, 4 dioxane on TS-SH and TS-SO_3H (a – d) (a) Freundlich, (b) Langmuir, and (c)Temkin,

(R^2 = 0.9963). The Langmuir removal capacity of TS-SO_3H for dioxane was found to be 164 mg/g. The K_L and 1/n values indicates that the feasible adsorption between the dioxane and the TS-SH or TS-SO_3H. The magnitude for the additional constants of the adsorption isotherms is listed in Table 2.

Table 2
Adsorption isotherms parameters for 1,4 dioxane on TS-SH and TS-SO_3H.

Freundlich	TS-SH	TS-SO_3H	Langmuir	TS-SH	TS-SO_3H	Temkin	TS-SH	TS-SO_3H
n	0.4953	1.010	$1/q_m$	0.0089	0.0061	A_T	2.21	2.95
1/n	2.0187	0.9902	q_m	112	164	B_T	20.1	23,1
K_f	0.2671	8.561	K_L	0.06	0.05	B	180.9	201
R^2	0.9954	0.9219	R^2	0.9802	0.9963	R^2	0.9852	0.9825

Table 3
Comparison of adsorption of 1, 4 dioxane adsorption on TS-SH and TS-SO_3H with other adsorbents.

Adsorbent	Q (mg/g)	Ref.
AC-A1	0.0652	[35]
AC-D	0.410	[35]
AC/TiO_2	0.33	[36]
Activated carbon/TiO_2	1.397	[37]
TS	85.17	[38]
TS-SH	112	This work
TS-SO_3H	164	This work

3.2.7. Adsorption mechanism

Both TS-SH and TS-SO_3H demonstrated a significant remediation of dioxane at neutral or slight basic medium. Because dioxane is a polar nonionic compound with two oxygen atoms, its high attachment might not have been attributable simply to hydrophobic combinations on the hydrophobic TS surface. 1,4-dioxane can develop intermolecular hydrogen bonds with the hydroxyl (OH), and sulfonic acid (SO_3H) moieties on the external surface of TS. The comparison of removal capacity of TS-SH and TS-SO_3H to other fabricated adsorbents is shown in Table 3.

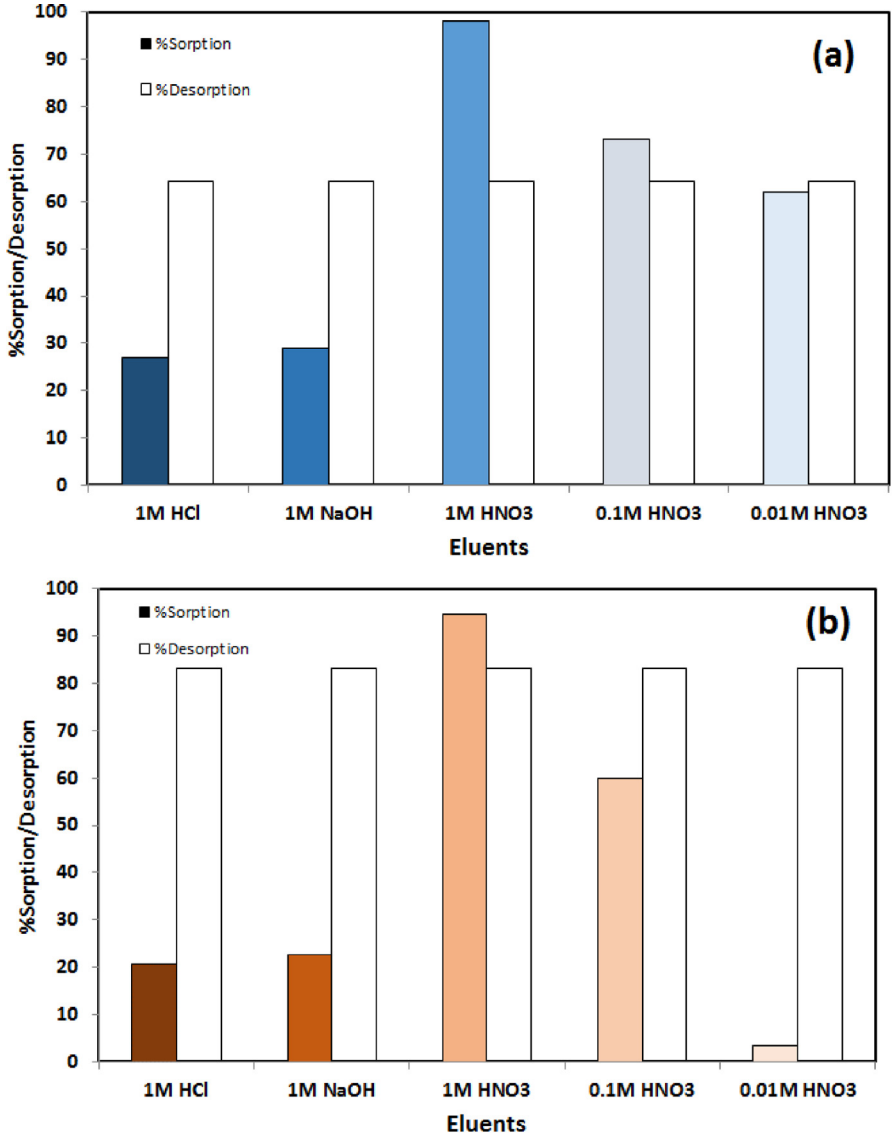

Fig. 10. . Desorption efficiency plots of 1,4 dioxane from (a) TS-SH and (b) TS-SO_3H by various eluents.

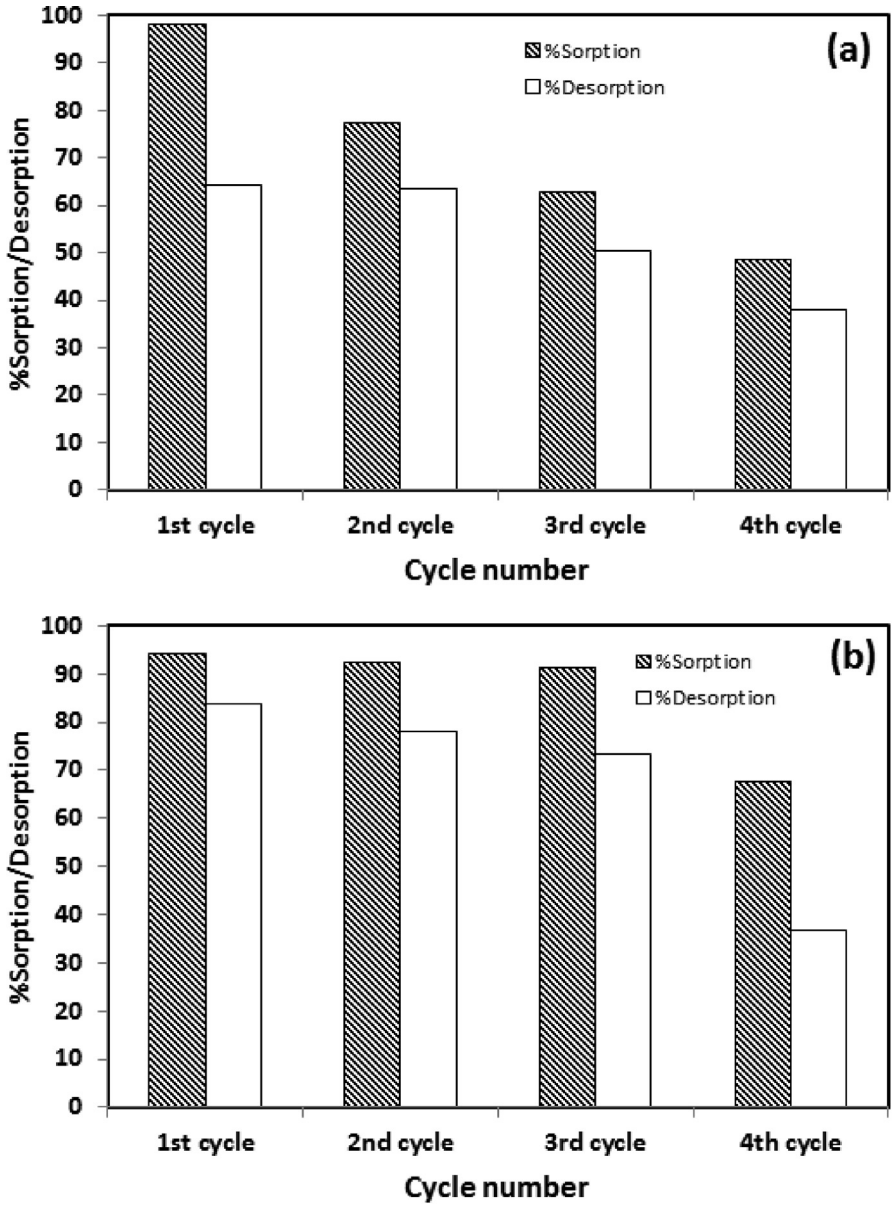

Fig. 11. . Adsorption and desorption cycles of (a) TS-SH and (b) TS-SO_3H.

3.2.8. Regeneration and reusability studies

Regeneration and durability are critical properties of modern adsorbent materials from economical point of view. The adsorption of dioxane onto the TS-SH and TS-SO_3H was minimal at smaller pH values, suggesting that the adsorbed dioxane may be detached from both adsorbents in an acidic medium. The detached studies were performed utilizing different acidic solutions; HCl (1 M), HNO_3 (1, 0.1, 0.01 M), and NaOH (1 M). The findings reveal that the HNO_3 (1 M) solution eluted easier than the nitrate due to the smaller the Cl^- ion sizes. A solution of HNO_3 (1 M) results in the best elution and recovery, as depicted in Fig. 10 for dioxane detached from both adsorbents. Furthermore, the dioxane desorption using low concentration of HNO_3 resulted in a considerable regeneration performance. The adsorption of dioxane on TS-SH and TS-SO_3H was 98%, 96% respectively, reduced to 50%, and 73% after four consecutive adsorption cycles. These results demonstrated that TS-SO_3H could sustain a large adsorption capacity during the fourth sorption–desorption run. Fig. 11.

4. Conclusion

For the first time, we developed scalable TS-SH and TS-SO_3H adsorbents for dioxane cleanup. These adsorbents demonstrated exceptional adsorption efficiency. Both adsorbents well obeyed the Langmuir adsorption isotherm and pseudo-second order model when removing dioxane. The maximum monolayer capacity (q_e) of TS-SH and TS-SO^3H were 112 mg g^{-1} and 164 mg g^{-1}, respectively, indicating that the produced adsorbents have a high potential for usage in removing hazardous organic chemicals from polluted water and industrial processes.

CRediT authorship contribution statement

Mohammed Saeed Alamri: Methodology, Investigation, Resources, Formal analysis, Writing – original draft, Software. **Hassan M.A. Hassan:** Conceptualization, Methodology, Investigation, Resources, Formal analysis, Supervision, Writing – review & edit-

ing. **Mosaed S. Alhumaimess:** Conceptualization, Methodology, Investigation, Formal analysis, Writing – original draft, Software, Validation, Writing – review & editing. **Abdullah M. Aldawsari:** Methodology, Investigation, Formal analysis, Validation. **Ahmed A. Alshahrani:** Investigation, Formal analysis, Validation. **Thamer S. Alraddadi:** Methodology, Investigation, Formal analysis, Validation. **Ibrahim Hotan Alsohaimi:** Conceptualization, Methodology, Investigation, Resources, Formal analysis, Writing – original draft, Software, Validation.

Declaration of Competing Interest

The authors declare that they have no known competing financial interests or personal relationships that could have appeared to influence the work reported in this paper.

Acknowledgement

The authors would like to thank the Deanship of graduate Studies at Jouf University for Funding and supporting this research through the initiative of DGS, Graduate Students Research Support (GSR) at Jouf University, Saudi Arabia.

References

[1] J.A. Stickney, S.L. Sager, J.R. Clarkson, L.A. Smith, B.J. Locey, M.J. Bock, R. Hartung, S.F. Olp, An updated evaluation of the carcinogenic potential of 1,4-dioxane, Regul. Toxicol. Pharmacol. 38 (2003) 183–195.
[2] M. Sun, C. Lopez-Velandia, D.R. Knappe, Determination of 1,4-dioxane in the Cape Fear River watershed by heated purge-and-trap preconcentration and gas chromatography– mass spectrometry, Environ. Sci. Technol. 50 (2016) 2246–2254.
[3] D.T. Adamson, S. Mahendra, K.L. Walker, S.R. Rauch, S. Sengupta, C.J. Newell, A multisite survey to identify the scale of the 1,4-dioxane problem at contaminated groundwater sites, Environ. Sci. Technol. Lett. 1 (2014) 254–258.
[4] T.K.G. Mohr, J.A. Stickney, W.H. DiGuiseppi, Environmental investigation and remediation: 1, 4-dioxane and other solvent stabilizers, first ed., CRC Press, Boca, Raton, 2016.
[5] S. Suthersan, J. Quinnan, J. Horst, I. Ross, E. Kalve, C. Bell, T. Pancras, Making strides in the management of "emerging contaminants", Ground. Water. Monit. R. 36 (2016) 15–25.
[6] S. Zhang, P.B. Gedalanga, S. Mahendra, Advances in bioremediation of 1,4-dioxane- contaminated waters, J. Environ. Manage. 204 (2017) 765–774.
[7] W. Li, E. Xu, D. Schlenk, H. Liu, Cyto-and geno-toxicity of 1,4-dioxane and its transformation products during ultraviolet-driven advanced oxidation processes, Environ. Sci.: Water Res. Technol. 4 (2018) 1213–1218.
[8] Y.T. Woo, B.J. Neuburger, J.C. Arcos, M.F. Argus, K. Nishiyama, G.W. Griffin, Enhancement of toxicity and enzyme-repressing activity of p-dioxane by chlorination: stereoselective effects, Toxicol. Lett. 5 (1980) 69–75.
[9] D.B. Miklos, C. Remy, M. Jekel, K.G. Linden, J.E. Drewes, U. Hubner, Evaluation of advanced oxidation processes for water and wastewater treatment–a critical review, Water Res. 139 (2018) 118–131.
[10] S. Mahendra, L. Alvarez-Cohen, Pseudonocardia dioxanivorans sp. nov., a novel actinomycete that grows on 1,4-dioxane, Int. J. Syst. Evol. Microbiol. 55 (2005) 593–598.
[11] S. Mahendra, L. Alvarez-Cohen, Kinetics of 1,4-dioxane biodegradation by monooxygenase-expressing bacteria, Environ. Sci. Technol. 40 (2006) 5435–5442.
[12] S. Mahendra, C.J. Petzold, E.E. Baidoo, J.D. Keasling, L. Alvarez-Cohen, Identification of the intermediates of in vivo oxidation of 1,4-dioxane by monooxygenase- containing bacteria, Environ. Sci. Technol. 41 (2007) 7330–7336.
[13] D. Inoue, T. Tsunoda, N. Yamamoto, M. Ike, K. Sei, 1,4-Dioxane degradation characteristics of Rhodococcus aetherivorans JCM 14343, Biodegradation 29 (2018) 301–310.
[14] A.L. Polasko, A. Zulli, P.B. Gedalanga, P. Pornwongthong, S. Mahendra, A mixed microbial community for the biodegradation of chlorinated ethenes and 1, 4-dioxane, Environ. Sci. Technol. Lett. 6 (2018) 49–54.
[15] S. Mahendra, A. Grostern, L. Alvarez-Cohen, The impact of chlorinated solvent cocontaminants on the biodegradation kinetics of 1,4-dioxane, Chemosphere 91 (2013) 88–92.
[16] C.S. Lee, C. Asato, M. Wang, X. Mao, C.J. Gobler, A.K. Venkatesan, Removal of 1, 4-dioxane during on-site wastewater treatment using nitrogen removing biofilters, Sci. Total Environ. 771 (2021) 144806.
[17] C. Dai, H. Wu, X. Wang, K. Zhao, Z. Lu, Network and meta-omics reveal the cooperation patterns and mechanisms in an efficient 1, 4-dioxane-degrading microbial consortium, Chemosphere 301 (2022) 134723.
[18] S.D. Patton, M.C. Dodd, H. Liu, Degradation of 1, 4-dioxane by reactive species generated during breakpoint chlorination: Proposed mechanisms and implications for water treatment and reuse. Journal of Hazardous, Mater. Lett. 3 (2022) 100054.
[19] W. Li, R. Xiao, H. Lin, K. Yang, K. He, L.H. Yang, S. Lv, Electro-activation of peroxymonosulfate by a graphene oxide/iron oxide nanoparticle-doped Ti_4O_7 ceramic membrane: mechanism of singlet oxygen generation in the removal of 1, 4-dioxane, J. Hazard. Mater. 424 (2022) 127342.
[20] G. Peregot, G. Bellussi, C. Corno, M. Taramasso, F. Buonomot, A. Esposito, Titanium-Silicalite: a novel derivative in the pentasil family, in: Y. Murakami, A. Iijima, J.W. Ward (Eds.), Studies in Surface Science and Catalysis, Elsevier, New York, 1986, pp. 129–136.
[21] X. Chen, P. Chen, H. Kita, Pervaporation through TS-1 membrane, Microporous Mesoporous Mater. 115 (2008) 164–169.
[22] D.P. Serrano, G. Calleja, J.A. Botas, F.J. Gutierrez, Characterization of adsorptive and hydrophobic properties of silicalite-1, ZSM-5, TS-1 and Beta zeolites by TPD techniques, Sep. Purif. Technol. 54 (2007) 1–9.
[23] C.F. Mellot, A.M. Davidson, J. Eckert, A.K. Cheetham, Adsorption of chloroform in NaY zeolite: a computational and vibrational spectroscopy study, J. Phys. Chem. B 102 (1998) 2530–2535.
[24] M. Taramasso, G. Perego, B. Notari, US 4410501, 1983.
[25] L. Wang, W. Liu, T. Wang, J. Ni, Highly efficient adsorption of Cr(VI) from aqueous solutions by amino-functionalized titanate nanotubes, Chem. Eng. J. 225 (2013) 153–163.
[26] H.M. Hassan, M.S. Alamri, A.N. Alrashidi, S.H. Mohamed, I.H. Alsohaimi, Validated spectrophotometric assessment of 1, 4-dioxane in drinking water by amionhydroxynaphthlene sulfonic acid (AHSA), Int. J. Environ. Anal. Chem. (2022) 1–11.
[27] Y. Jun, H. Zarrin, M. Fowler, Z. Chen, Functionalized titania nanotube composite membranes for high temperature proton exchange membrane fuel cells, Int. J. Hydrogen Energy 36 (2011) 6073–6081.
[28] L. Dal Pozzo, G. Fornasari, T. Monti, TS-1, catalytic mechanism in cyclohexanoneoxime production, Catal. Commun. 3 (2002) 369–375.
[29] D.M. Marzouqa, M.B. Zughul, M.O. Taha, H.A. Hodali, Effect of particle morphology and pore size on the release kinetics of ephedrine from mesoporous MCM-41 materials, J. Porous Mater. 19 (2012) 825–833.
[30] F. Wakabayashi, J.N. Kondo, K. Domen, C. Hirose, FT-IR study of H2 18O adsorption on H-ZSM-5: direct evidence for the hydrogen-bonded adsorption of water, J. Phys. Chem. 100 (1996) 1442–1444.
[31] T. Xue, H. Liu, Y. Wang, H. Wu, P. Wu, M. He, Seedinduced synthesis of small-crystal TS-1 using ammonia as alkali source, Chin. J. Catal. 36 (11) (2015) 1928–1935.
[32] G. Ricchiardi, A. Damin, S. Bordiga, et al., Vibrational Structure of Titanium Silicate Catalysts. A Spectroscopic and Theoretical Study, J. Am. Chem. Soc. 123 (2001) 11409–11419.
[33] Y.B. Onundi, A.A. Mamun, M.F. Al Khatib, Y.M. Ahmed, Adsorption of copper, nickel and lead ions from synthetic semiconductor industrial wastewater by palm shell activated carbon, Int. J. Environ. Sci. Tech. 7 (2010) 751–758.
[34] G. Moussavi, M. Mahmoudi, Removal of azo and anthraquinone reactive dyes from industrial wastewaters using MgO nanoparticles, J. Hazard. Mater. 168 (2009) 806–812.
[35] T. Fukuhara, S. Iwasaki, T. Hasegawa, K. Ishihara, M. Fujiwara, I. Abe, Adsorption of 1, 4-Dioxane from Aqueous Solutions onto Various Activated Carbons, J. Water Environ. Techn. 9 (3) (2011) 249–258.
[36] Y. Nomura, S. Fukahori, T. Fujiwara, Removal of 1, 4-dioxane from landfill leachate by a rotating advanced oxidation contactor equipped with activated carbon/TiO2 composite sheets, J.hazard. Mater. 383 (2020) 121005.
[37] Y. Nomura, S. Fukahori, Y. Shiozawa, T. Fujiwara, Adsorptive removal and photocatalytic decomposition of 1,4-dioxane in landfill leachate using activated carbon/TiO2 composites. J. Japan Soc. Civ. Eng. Ser. G (2016) (Environ. Res. 72, III_419–III_427).
[38] R. Chen, C. Liu, N.W. Johnson, L. Zhang, S. Mahendra, Y. Liu, M. Chen, Removal of 1, 4-dioxane by titanium silicalite-1: Separation mechanisms and bioregeneration of sorption sites, Chem. Eng. J. 371 (2019) 193–202.